

## Noninvasive metal contacts in chemically derived graphene devices

Ravi S. Sundaram, Cristina Gomez-Navarro, Eduardo J. H. Lee, Marko Burghard, and Klaus Kern

Citation: *Appl. Phys. Lett.* **95**, 223507 (2009); doi: 10.1063/1.3270533

View online: <http://dx.doi.org/10.1063/1.3270533>

View Table of Contents: <http://apl.aip.org/resource/1/APPLAB/v95/i22>

Published by the [American Institute of Physics](http://www.aip.org).

---

### Related Articles

Ohmic contacts to n-type germanium with low specific contact resistivity  
*Appl. Phys. Lett.* **100**, 022113 (2012)

Ultrasensitive anomalous Hall effect in SiO<sub>2</sub>/Fe-Pt/SiO<sub>2</sub> sandwich structure films  
*Appl. Phys. Lett.* **100**, 022404 (2012)

Antiferromagnetic coupling across silicon regulated by tunneling currents  
*Appl. Phys. Lett.* **100**, 022406 (2012)

Tuning the Schottky barrier height at MgO/metal interface  
*Appl. Phys. Lett.* **100**, 022103 (2012)

Three-dimensional shaping of sub-micron GaAs Schottky junctions for zero-bias terahertz rectification  
*Appl. Phys. Lett.* **99**, 263505 (2011)

---

### Additional information on *Appl. Phys. Lett.*

Journal Homepage: <http://apl.aip.org/>

Journal Information: [http://apl.aip.org/about/about\\_the\\_journal](http://apl.aip.org/about/about_the_journal)

Top downloads: [http://apl.aip.org/features/most\\_downloaded](http://apl.aip.org/features/most_downloaded)

Information for Authors: <http://apl.aip.org/authors>

### ADVERTISEMENT

The logo for AIP Advances features the text 'AIP Advances' in a blue and green font. Above the text is a decorative graphic of several orange and yellow circles of varying sizes, some connected by a dotted line, suggesting a molecular or atomic structure.

*Submit Now*

Explore AIP's new  
open-access journal

- Article-level metrics now available
- Join the conversation! Rate & comment on articles

## Noninvasive metal contacts in chemically derived graphene devices

Ravi S. Sundaram,<sup>1,a)</sup> Cristina Gomez-Navarro,<sup>1,2,a)</sup> Eduardo J. H. Lee,<sup>1</sup> Marko Burghard,<sup>1</sup> and Klaus Kern<sup>1,3</sup>

<sup>1</sup>Max Planck Institut fuer Festkoerperforschung, Heisenbergstrasse 1, Stuttgart 70569, Germany

<sup>2</sup>Departamento de Física de la Materia Condensada, Universidad Autónoma de Madrid, Madrid 28049, Spain

<sup>3</sup>Institut de Physique de la Matière Condensée, Ecole Polytechnique Fédérale de Lausanne, Lausanne CH-1015, Switzerland

(Received 26 June 2009; accepted 9 November 2009; published online 4 December 2009)

We study the properties of gold contacts on chemically derived graphene devices by scanning photocurrent microscopy and gate-dependent electrical transport measurements. In the as-fabricated devices, negligible potential barriers are found at the gold/graphene interface, reflecting the noninvasive character of the contacts. Device annealing above 300 °C leads to the formation of potential barriers at the contacts concomitant with metal-induced *p*-type doping of the sheet as a consequence of the diffusion of gold from the electrodes. The transfer characteristics of the chemically derived graphene devices point toward the suppression of Klein tunneling in this material. © 2009 American Institute of Physics. [doi:10.1063/1.3270533]

The performance of nanoelectronic devices based on carbon nanostructures is strongly governed by the properties of the implemented electrical contacts.<sup>1</sup> In the early stages of carbon nanotube research, the poor quality of the metal contacts impeded the exploration of intriguing phenomena such as ballistic conduction or spin injection. Later on, metals such as palladium were found to provide close-to-ideal contacts, which enabled the realization of ballistic field-effect transistors (FETs) from individual single-wall carbon nanotubes.<sup>2</sup> Moreover, the availability of suitable ferromagnetic metal contacts led to the development of spin valves incorporating carbon nanotubes.<sup>3</sup> More recently, experimental studies of metal contacts on mechanically exfoliated graphene sheets have revealed the presence of local doping under the metal contacts,<sup>4</sup> a finding in accordance with theoretical investigations.<sup>5</sup> It has also been experimentally observed that the magnitude of the resulting potential step is dependant on the difference in work function of graphene and the contact metal.<sup>6</sup>

The charge transfer at the graphene-metal interface leads to a charge inhomogeneity that surrounds the metal contacts and extends to considerable distances inside the graphene channel, which manifests itself in a notable asymmetry between electron and hole conductance in such devices.<sup>6</sup> Moreover, the invasiveness of the metal contacts on graphene can notably influence electrical measurements even in the four-probe geometry.<sup>7</sup> Here we demonstrate that noninvasive metal contacts can be realized on chemically derived graphene obtained through the graphite oxide route.<sup>8,9</sup> This synthesis approach affords a high yield of graphene oxide (GO) monolayers which are then chemically reduced to remove the majority of the contained oxygenated functional groups.<sup>9–12</sup> Substantial progress has recently been made toward approaching the electrical performance of exfoliated graphene.<sup>11,13,14</sup> Compared to micromechanical cleavage, the chemical synthesis of graphene offers several advantages for various applications in nanoelectronics, in-

cluding the possibility to deposit high densities of large monolayers on technologically relevant substrates.<sup>9,15</sup> In addition, GO is a promising starting material for integrated devices wherein the electrically active graphene regions are separated by carbon oxide barriers.<sup>16</sup> In the present work, we examine the properties of gold contacts on chemically reduced GO (RGO) monolayers by the combination of electrical transport measurements with scanning photocurrent microscopy (SPCM). The latter technique has proven to be a valuable tool for mapping built-in electric fields in devices based on individual carbon nanotubes<sup>17</sup> or exfoliated graphene.<sup>4</sup>

Graphite oxide was prepared starting from graphite flakes according to Hummers method.<sup>18</sup> After dispersing the resulting powder in water with the aid of ultrasonication, it was deposited on a Si substrate covered with a 300 nm thick thermally grown SiO<sub>2</sub> layer which was modified by 3-(aminopropyl)-triethoxysilane prior to deposition. The deposited GO monolayers with sizes of  $\sim 20 \times 20 \mu\text{m}^2$  were then etched using oxygen plasma (200 W, 0.3 Torr, 15 s), followed by chemical reduction through two subsequent steps comprising hydrogen plasma treatment (0.8 mbar H<sub>2</sub> at 30 W power for  $\sim 6$  s) and thermal annealing (by inserting sample in a preheated furnace at 400 °C for 1 h). Individual reduced and annealed GO monolayers with heights of  $\sim 1$  nm, as identified by atomic force microscopy (AFM), were contacted with Ti/Au (1 nm/30 nm) electrodes via a standard e-beam lithography process [Fig. 1(a)], resulting in a bottom-gated FET configuration. SPCM measurements were performed using a diffraction-limited laser spot ( $\lambda = 514$  nm, spot size  $\sim 0.4 \mu\text{m}$ , power  $\sim 100 \text{ kW cm}^{-2}$ ). For spatial correlation of the photocurrent response, the optical reflection and photocurrent were acquired simultaneously. The acquired AFM, reflection, and photocurrent images were processed using the WSXM software.<sup>19</sup>

Electrical characterization of the as-fabricated RGO devices revealed two-probe resistances of 4–7 M $\Omega$  under ambient conditions. This range is in good agreement with previous results obtained from RGO monolayers contacted by AuPd electrodes.<sup>9,20</sup> The reflection image of a device with

<sup>a)</sup>Authors to whom correspondence should be addressed. Electronic addresses: r.sundaram@fkf.mpg.de and cristina.gomez@uam.es.

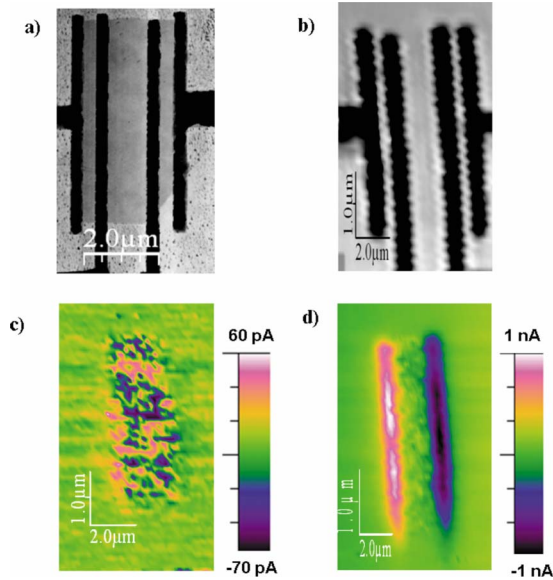


FIG. 1. (Color online) (a) AFM tapping mode image of an RGO layer contacted with 4 probes of Ti(1 nm)/Au(30 nm). (b) Reflection image measured during the acquisition of the photocurrent images for spatial correlation. [(c) and (d)] Photocurrent images taken at  $V_{ds}=V_{gs}=0$  V of the as-fabricated and annealed device (at  $\sim 300$  °C), respectively.

four electrodes is depicted in Fig. 1(b), while Fig. 1(c) depicts the corresponding SPCM image recorded at zero source drain and gate bias. The latter image reveals numerous spots of fluctuating sign throughout the sheet. This signal pattern, which showed only a weak modulation upon sweeping the back gate voltage between  $\pm 60$  V, reflects surface potential variations that may arise from defective  $sp^3$ -hybridized regions remaining after the chemical reduction,<sup>9,21,22</sup> or from charged impurities located on the substrate akin to signatures of electron-hole puddles in SPCM images of pristine graphene.<sup>4,23</sup> The photocurrent distribution in the as-fabricated devices clearly differs from exfoliated graphene with evaporated gold contacts<sup>4,23</sup> by the absence of distinguishable signals at the contacts. It thus follows that no appreciable potential barriers are present at the interface between gold and the RGO, resulting in noninvasive contacts. This conclusion is corroborated by the fact that four-probe and two-probe electrical measurements on the devices yielded approximately the same resistance. The absence of potential barriers may be attributed to the substantial density of defects (e.g., remaining oxygen-containing functional groups) contained in the RGO,<sup>21,22</sup> which block the formation of an intimate gold-graphene interface. In order to test this hypothesis, we investigated the effect of annealing on the contact properties of the RGO devices. We found that a treatment above 300 °C (for 1 h under argon atmosphere) causes a significant change in the SPCM response, specifically the emergence of pronounced photocurrent signals close to the contacts, indicative of the creation of local potential barriers [Fig. 1(d)]. This change thus signifies the annealing-induced formation of intimate contacts of gold with carbon and the subsequent transfer of charge at the gold-carbon interface.

As a further change after annealing, the transfer characteristics measured under a He atmosphere display a shift in the current minimum (i.e., Dirac point) toward more positive gate voltages by  $\sim 60$  V [Fig. 2(a)]. Such positive shift is

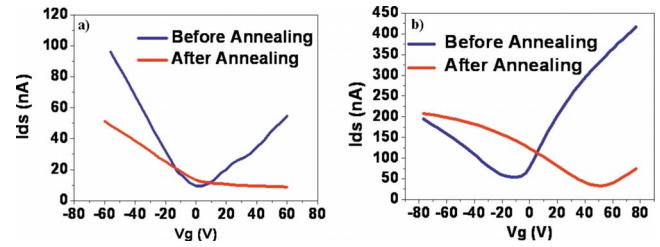


FIG. 2. (Color online) (a) Transfer characteristics ( $I_{ds}$ - $V_g$  curves) of an RGO device measured at 100 mV bias under helium atmosphere at 240 K before and after annealing at 300 °C. (b) Comparison of the transfer characteristics (acquired at  $V_{bias}=1$  mV) of a micromechanically exfoliated graphene device before and after annealing under the same conditions as in panel (a).

indicative of  $p$ -type doping of the RGO channel. The sheet doping is likely to originate from the lateral diffusion of gold atoms from the contacts along the RGO sheet during the annealing process. Noble metal-induced  $p$ -type doping of graphene has been documented for gold-decorated epitaxial graphene upon annealing.<sup>24</sup> A similar doping effect, as manifested in a pronounced positive shift in the Dirac point, could also be observed for gold-contacted micromechanically exfoliated graphene after annealing under the same conditions [Fig. 2(b)]. However, while in the latter case the slope of the hole branch (for not too negative gate voltages) remains largely unaltered, it is strongly reduced in the RGO device. One plausible explanation for this difference involves reduced Klein tunneling in the disordered RGO, which would impede the charge transport through the potential barriers formed between the  $p$ -doped contact regions and the central RGO channel whose Fermi level position is modulated by the applied back gate voltage [Fig. 3(a)]. The suppression of Klein tunneling by the presence of disorder in graphene has been predicted by theory.<sup>25</sup> Support for the relevance of this effect in the annealed RGO devices derives from the finding of an increasingly suppressed slope of the hole branch with the magnitude of the photocurrent signal detected close to one of the contacts, as is apparent from the plots in Fig. 3(b) belonging to three different RGO devices that reflect the sample-to-sample variation despite their identical treatments. Such trend would be expected on the basis that the photocurrent signal is proportional to the local electric potential gradient. It is interesting to note that for the RGO devices at  $V_g=0$  V, the resistance increase due to the suppression of Klein tunneling is roughly compensated by the resistance

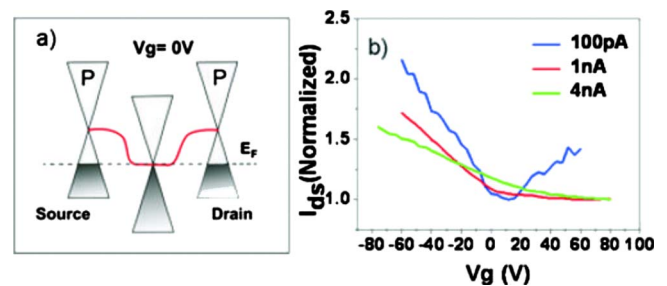


FIG. 3. (Color online) (a) Schematic representation of the potential barriers formed within an annealed RGO device at zero back gate voltage. Upon application of a back gate voltage, the Fermi level of the  $p$ -doped regions close to the gold contacts would remain pinned, while it would be shifted within the central graphene channel. (b) Transfer characteristics of three different RGO devices (after annealing at 300 °C) exhibiting different magnitudes of the photocurrent signals detected close to one of the electrodes.

decrease due to gold-induced *p*-type doping, whereas the latter effect is predominant in the exfoliated graphene device which accordingly displays a resistance decrease at  $V_g = 0$  V (Fig. 2).

In summary, our data provide evidence for the inherent defective nature of chemically derived graphene prepared by the GO route due to which the direct evaporation of gold results in noninvasive contacts characterized by the absence of potential steps. This behavior is in contrast to exfoliated graphene, wherein metal contacts principally generate macroscopic charge inhomogeneities which interfere with four-probe measurements. At only moderately high temperatures, both types of graphene are prone to diffusion of gold atoms from the contacts, a property that should be considered in the future fabrication of graphene-based devices.

The authors acknowledge Dr. Yan Yu Liang and Dr. Xinliang Feng from Max Planck Institute for Polymer Research, Mainz for providing high quality GO suspensions.

- <sup>1</sup>Z. Chen, J. Appenzeller, J. Knoch, Y.-m. Lin, and P. Avouris, *Nano Lett.* **5**, 1497 (2005).
- <sup>2</sup>A. Javey, J. Guo, Q. Wang, M. Lundstrom, and H. Dai, *Nature (London)* **424**, 654 (2003).
- <sup>3</sup>S. Sahoo, T. Kontos, C. Schonenberger, and C. Surlers, *Appl. Phys. Lett.* **86**, 112109 (2005).
- <sup>4</sup>E. J. H. Lee, K. Balasubramanian, R. T. Weitz, M. Burghard, and K. Kern, *Nat. Nanotechnol.* **3**, 486 (2008).
- <sup>5</sup>G. Giovannetti, P. A. Khomyakov, G. Brocks, V. M. Karpan, J. van den Brink, and P. J. Kelly, *Phys. Rev. Lett.* **101**, 026803 (2008).
- <sup>6</sup>B. Huard, N. Stander, J. A. Sulpizio, and D. Goldhaber-Gordon, *Phys. Rev. B* **78**, 121402 (2008).
- <sup>7</sup>B. Gao, Y. F. Chen, M. S. Fuhrer, D. C. Glatli, and A. Bachtold, *Phys. Rev. Lett.* **95**, 196802 (2005).
- <sup>8</sup>S. Stankovich, D. A. Dikin, G. H. B. Dommett, K. M. Kohlhaas, E. J. Zimney, E. A. Stach, R. D. Piner, S. T. Nguyen, and R. S. Ruoff, *Nature (London)* **442**, 282 (2006).
- <sup>9</sup>C. Gómez-Navarro, R. T. Weitz, A. M. Bittner, M. Scolari, A. Mews, M. Burghard, and K. Kern, *Nano Lett.* **7**, 3499 (2007).
- <sup>10</sup>Y. Hernandez, V. Nicolosi, M. Lotya, F. M. Blighe, Z. Y. Sun, S. De, I. T. McGovern, B. Holland, M. Byrne, Y. K. Gun'ko, J. J. Boland, P. Niraj, G. Duesberg, S. Krishnamurthy, R. Goodhue, J. Hutchison, V. Scardaci, A. C. Ferrari, and J. N. Coleman, *Nat. Nanotechnol.* **3**, 563 (2008).
- <sup>11</sup>V. C. Tung, M. J. Allen, Y. Yang, and R. B. Kaner, *Nat. Nanotechnol.* **4**, 25 (2009).
- <sup>12</sup>A. Reina, X. Jia, J. Ho, D. Nezich, H. Son, V. Bulovic, M. S. Dresselhaus, and J. Kong, *Nano Lett.* **9**, 30 (2009).
- <sup>13</sup>I. Jung, D. A. Dikin, R. D. Piner, and R. S. Ruoff, *Nano Lett.* **8**, 4283 (2008).
- <sup>14</sup>D. Li, M. B. Muller, S. Gilje, R. B. Kaner, and G. G. Wallace, *Nat. Nanotechnol.* **3**, 101 (2008).
- <sup>15</sup>S. Gilje, S. Han, W. Minsheng, L. W. Kang, and R. B. Kaner, *Nano Lett.* **7**, 3394 (2007).
- <sup>16</sup>X. S. Wu, M. Sprinkle, X. B. Li, F. Ming, C. Berger, and W. A. de Heer, *Phys. Rev. Lett.* **101**, 026801 (2008).
- <sup>17</sup>E. J. H. Lee, K. Balasubramanian, J. Dorfmueller, R. Vogelgesang, N. Fu, A. Mews, M. Burghard, and K. Kern, *Small* **3**, 2038 (2007).
- <sup>18</sup>W. S. Hummers and R. E. Offeman, *J. Am. Chem. Soc.* **80**, 1339 (1958).
- <sup>19</sup>I. Horcas, R. Fernandez, J. M. Gomez-Rodriguez, J. Colchero, J. Gomez-Herrero, and A. M. Baro, *Rev. Sci. Instrum.* **78**, 013705 (2007).
- <sup>20</sup>R. S. Sundaram, C. Gómez-Navarro, K. Balasubramanian, M. Burghard, and K. Kern, *Adv. Mater.* **20**, 3050 (2008).
- <sup>21</sup>T. Szabó, O. Berkesi, P. Forgo, K. Josepovits, Y. Sanakis, D. Petridis, and I. Dekany, *Chem. Mater.* **18**, 2740 (2006).
- <sup>22</sup>W. W. Cai, R. D. Piner, F. J. Stadermann, S. Park, M. A. Shaibat, Y. Ishii, D. X. Yang, A. Velamakanni, S. J. An, M. Stoller, J. H. An, D. M. Chen, and R. S. Ruoff, *Science* **321**, 1815 (2008).
- <sup>23</sup>F. Xia, T. Mueller, R. Golizadeh-Mojarad, M. Freitag, Y.-m. Lin, J. Tsang, V. Perebeinos, and P. Avouris, *Nano Lett.* **9**, 1039 (2009).
- <sup>24</sup>T. Gierz, C. Riedl, U. Starke, C. R. Ast, and K. Kern, *Nano Lett.* **8**, 4603 (2008).
- <sup>25</sup>M. M. Fogler, D. S. Novikov, L. I. Glazman, and B. I. Shklovskii, *Phys. Rev. B* **77**, 075420 (2008).